

Probing the Mechanochemistry of Metal–Organic Frameworks with Low-Frequency Vibrational Spectroscopy

Wei Zhang,^{†,#} Jefferson Maul,^{‡,#} Diana Vulpe,[§] Peyman Z. Moghadam,^{||} David Fairen-Jimenez,[§] Daniel M. Mittleman,[†] J. Axel Zeitler,[§] Alessandro Erba,^{*,‡} and Michael T. Ruggiero^{*,§,⊥}

[†]School of Engineering, Brown University, 184 Hope St., Providence, Rhode Island 02912, United States

[‡]Dipartimento di Chimica, Università di Torino, via Giuria 5, 10125 Torino, Italy

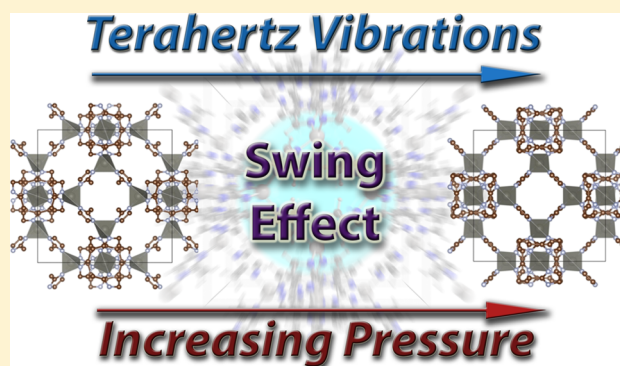
[§]Department of Chemical Engineering and Biotechnology, University of Cambridge, Philippa Fawcett Drive, Cambridge CB3 0AS, United Kingdom

^{||}Department of Chemical and Biological Engineering, University of Sheffield, Mappin Street, Sheffield S1 3JD, United Kingdom

[⊥]Department of Chemistry, University of Vermont, 82 University Place, Burlington, Vermont 05405, United States

Supporting Information

ABSTRACT: The identification and characterization of low-frequency vibrational motions of metal–organic frameworks (MOFs) allows for a better understanding of their mechanical and structural response upon perturbation by external stimuli such as temperature, pressure, and adsorption. Here, we describe the combination of temperature- and pressure-dependent terahertz spectroscopy measurements with quantum mechanical simulations to measure and assign specific low-frequency vibrational modes that directly drive the mechanochemical properties of this important class of porous materials. More specifically, we identify intense spectral features in the terahertz region of the vibrational spectrum of ZIF-8 which are directly connected to its mechanochemical response. In particular, we find that the mechanical compressibility of pristine ZIF-8 follows a peculiar nonlinear trend upon pressure: its bulk modulus initially increases up to 0.1 GPa and decreases at higher pressures, which is simultaneously reflected in the terahertz vibrational spectra. This work highlights the interplay between structural, vibrational, and mechanochemical phenomena, all of which are key to the effective exploitation of MOFs. The importance of terahertz vibrational motions on the function of MOFs is demonstrated, and a method is presented for their measurement and interpretation, which can be applied widely to any supramolecular material.



INTRODUCTION

The connections between low-frequency large-amplitude terahertz vibrations and material function are becoming increasingly apparent. These motions have been shown to play a critical role in enzymatic catalysis and ligand binding, vibrational dampening and relaxation, crystallization and amorphization phenomena, phase transitions, structural response to temperature and pressure (e.g., negative thermal expansion), and so forth.^{1–7} Recently, Ryder et al. have analyzed the low-frequency lattice dynamics of metal–organic frameworks (MOFs) and suggested that they can play an important role into their proper function and behavior; however no explicit connection between these phenomena has been established beyond inference (based on spectral assignment).^{8,9} In this respect, the current challenge is that of establishing an explicit link between specific terahertz lattice vibrations and specific MOF functionalities, which would increase their effective design and use.

MOFs are a promising class of porous materials owing to their intrinsic structural and mechanical properties and large specific surface areas. They have been proposed for industrial applications such as energy storage, drug delivery, catalysis, and chemical separation.^{10–15} MOFs can be readily tuned through the modification of either the metal cluster or organic linkers, leading to a virtually infinite number of materials that are yet to be fully explored.^{16,17} The diversity found in MOFs brings a unique combination of structural, chemical, and mechanical properties that play a critical role in their behavior and performance. So far, little attention has been paid to the role that the nuclear dynamics, particularly the low-frequency dynamics, has on these phenomena.

Among the existing MOFs that can be studied, ZIF-8 (ZIF: zeolitic imidazolate framework) is a prototypical example that

Received: August 27, 2018

Revised: November 6, 2018

Published: November 6, 2018

has been widely investigated, for which two crystalline phases and an amorphous phase have been reported.^{18–20} Importantly, these two crystalline phases are characterized by a critical change in pore size and accessibility. Moggach et al. described a first-order adsorption-induced phase transition at 1.47 GPa when using methanol as a pressure-transmitting medium (PTM) under hydrostatic conditions;²⁰ when using a nonpenetrating fluid as the PTM (i.e., no guest molecules in the cavities), a pressure-induced amorphization was observed at 0.34 GPa.¹⁹ In recent years, a number of studies, both experimental and theoretical, have been performed to study the role of pressure, temperature, and the nature of the gas molecules on the adsorption capacity of ZIF-8, including the apparently counterintuitive case of an increased pore window size upon pressure.^{20–25} More specifically, using both in situ powder X-ray diffraction and molecular simulation, it has been shown that a “gate-opening” or “swing-effect” adsorption-induced structural change occurs in ZIF-8 at much lower pressures, where—similar to the 1.47 GPa phase described above—the imidazolate linkers rotate so as to increase the size of the accessible pore window.^{21,26,27} These classes of motions, i.e. large-amplitude displacements of entire molecular subunits, occur at terahertz frequencies,²⁸ confirming that terahertz vibrations play a key role in the mechanochemical properties and phase-transition pathways present in such solids.

Low-frequency vibrational spectroscopies have been used to study ZIFs,^{9,29} providing valuable information related to the specific vibrational motions that are present, as well as for the detection of gas-adsorption in ZIF-8.³⁰ Terahertz time-domain spectroscopy (THz-TDS) can be used to acquire experimental spectra of infrared-active vibrational modes in the far-infrared. Compared to traditional far-infrared spectroscopy, the method is convenient in that it can collect high-quality spectra within seconds with signal-to-noise characteristics far exceeding that of Fourier transform instruments.³¹ THz-TDS is particularly useful for the investigation of ZIFs because it directly probes large-amplitude collective atomic motions that are expected in the terahertz frequency range (0.1–10 THz, 3–333 cm⁻¹). These vibrations are strongly dependent on both the intermolecular and intramolecular potential energy landscape, and thus THz-TDS is a sensitive probe of all the interactions present within solids. While the relationship between lattice dynamics and mechanochemical phenomena has been clearly long established,^{32,33} recent work in the MOF community has focused on identifying specific low-frequency vibrational modes that might be relevant to the elastic response of such materials.^{8,9} For the MOF community, these exploratory studies have very usefully directed attention toward considering the well-known relationship between the terahertz (lattice) vibrations and mechanical properties. However, given the proof-of-concept nature of those studies, the conclusions drawn were necessarily based on the qualitative inspection of the vibrational mode types, with emphasis on motions that were considered to involve pathways corresponding to particular deformations (e.g., shear deformation). A quantitative analysis of the mechanisms was not possible as the experimental data were largely based on inelastic neutron scattering and synchrotron far-infrared measurements, techniques that, in contrast to THz-TDS, unfortunately exhibit a dramatic reduction in the signal-to-noise ratio at the low-frequencies (<100 cm⁻¹), data which are critical to obtain quantitative insight.

Here, we discuss the interplay between pressure-induced structural, dynamical, and mechanical intrinsic features of a relatively flexible MOF:ZIF-8. In particular, we establish the relationship between specific low-frequency vibrational modes and the mechanochemical response of the material in the presence of external perturbations.

We propose a combination of experimental pressure- and temperature-dependent THz-TDS and quantum-mechanical simulations to provide a consistent description of ZIF-8 upon compression. A peculiar nonlinear pressure-dependence of the bulk modulus of ZIF-8 before amorphization is reported. We also describe the use of an innovative way to probe the effects of pressure and adsorption on the structure and dynamics of MOF systems, specifically when using gases that will adsorb, by combining in situ THz-TDS with a pressurized sample cell. Although we focus on ZIF-8, this approach can be extended to other MOFs and supramolecular materials in general.

■ MATERIALS AND METHODS

Quantum-Mechanical Simulations. *Solid-State DFT.* The CRYSTAL17 software package was used for all solid-state density-functional-theory calculations.³⁴ All simulations utilized the M06-2X density functional³⁵ coupled with the all-electron double- ζ 6-31G(d,p) basis set due to previous success.²⁹ Atomic positions were initialized from the experimentally determined single-crystal X-ray diffraction structure³⁶ and were optimized at several pressures without any symmetry constraints by adding a diagonal hydrostatic prestress to the analytical stress tensor.³⁷ It is important to note that due to ZIF-8 undergoing a phase-transition within the same space group ($\bar{1}43m \rightarrow \bar{1}43m$) when using a penetrating PTM, identical results were obtained when performing simulations within the constraint of space group symmetry, as well as without any symmetry. Vibrational simulations were performed within the harmonic approximation via numerical differentiation (with atomic displacements of 0.003 Å),³⁸ and IR intensities were determined using the Berry phase method. Energy convergence criteria were set to $\Delta E \leq 10^{-10}$ hartree for both optimizations and frequency calculations. A shrinking factor of 4 is used for all calculations, corresponding to a $4 \times 4 \times 4$ mesh of k points and to 36 or 8 k points in the symmetry-irreducible Brillouin zone without or with exploitation of the space group symmetry, respectively, and convergence was checked by performing single-point energy calculations at various k point samplings.

Ab Initio Molecular Dynamics. The open-source CP2K software package was used for all ab initio molecular dynamics (AIMD) simulations.³⁹ Initially, 48 nitrogen molecules were randomly placed within the pore of the ZIF-8 crystal based on a minimum van der Waals radii method. Subsequently, both the loaded and unloaded crystals were simulated within the canonical (NVT) ensemble and the temperature was maintained at 100 K using a Nosé–Hoover chain thermostat.⁴⁰ Unfortunately, CP2K does not have the meta-GGA functionals available, and therefore the Perdew–Burke–Ernzerhof density functional⁴¹ was coupled with the double- ζ DZVP basis set⁴² and Goedecker–Teter–Hutter pseudopotentials,⁴³ with the D3-dispersion correction (with the Becke–Johnson damping functional) applied to all models.⁴⁴ The energy convergence criterion was set to be $\Delta E < 10^{-9}$ hartree. The systems were equilibrated for 10 ps prior to performing the simulations for vibrational analysis. IR spectra were generated by taking the Fourier transform of the dipole moment autocorrelation

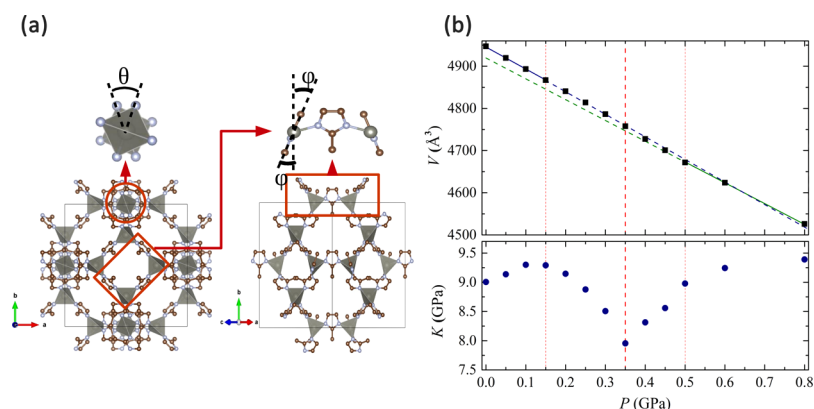


Figure 1. (a) Structure of ZIF-8; two angles φ and θ are graphically defined, which represent the rotation of the imidazolate linkers and the twisting of the ZnN_4 tetrahedra, respectively. (b) DFT-predicted volume V and bulk modulus K as a function of pressure in the low-pressure regime. Red dashed lines are eye-guides to identify three different structural trends, while the solid blue and green lines represent linear fits to the low- and high-pressure regions, respectively, with dashed lines representing the extrapolated curves.

function, and all post-processing was performed using the TRAVIS software package.⁴⁵ A 0.5 fs time step was used, and the molecular dipole moments were determined every 2.5 fs via determination of the Wannier centers.⁴⁶ The spectra presented are obtained from a 30 ps trajectory, which has previously been shown to be sufficient for the vibrational analyses of molecular crystals.⁴⁶

Terahertz Time-Domain Spectroscopy. ZIF-8 sample (30–35 mg) was mixed with 360 mg of high density polyethylene (PE) and compressed into tablets with diameters of 6 mm and thicknesses of 2.5 mm and then placed into a custom-made pressure cell. No apparent amorphization occurred during the sample preparation due to the observation of a clear crystalline THz-TDS spectrum, as opposed to the featureless absorption expected of an amorphous solid. High-pressure compressed gases (methane and nitrogen) were guided into the pressure cell to pressurize the sample tablet, and a liquid nitrogen cold finger and an electric heater were used to accurately control the sample temperature. The details regarding the operation of the pressure cell were previously reported.⁴⁷ For each scan, we fixed the pressure and down-scanned the temperature from 300 K with a rate of 0.47 K/min.

A custom-made THz time-domain spectrometer was used to record the time-domain waveforms of the THz radiation that transmitted through the sample.⁴⁷ The time-domain waveforms were truncated with an asymmetric tapered cosine window with a length of approximately 16 ps to keep only the main THz pulse and then zero-padded and Fourier-transformed to obtain the spectra. The spectrum of a pure PE tablet was also measured, as the reference. The frequencies and linewidths of the modes were obtained by fitting the spectra to the sum of two Gaussian lineshapes $e^{-(f-f_i)/2\sigma_i^2}$ on top of a quadratic background $af^2 + b$, where f is the frequency, f_i is the central frequency of the i -th mode, $\sqrt{2 \ln 2} \sigma_i$ is the half width at half-maximum of the i -th mode, and a and b are coefficients for the quadratic background.

RESULTS AND DISCUSSION

Origin of Anomalous Low-Pressure Mechanical Properties. The relationship between pressure-dependent properties and performance of porous materials is of critical importance in applications such as in gas-storage and

sequestration materials. Taking ZIF-8—with a cubic lattice ($I43m$)—as an example of a flexible MOF, several seemingly anomalous pressure-dependent features have been reported in the last few years. This is including the observation of (i) increasing pore accessibility with pressure,²⁰ (ii) a negative value for the pressure derivative of the bulk modulus K (i.e. K') in the low pressure regime—suggesting the softening of the mechanical response of the system upon pressure,¹⁹ and (iii) an intrinsic amorphization above pressures of 0.34 GPa when using a nonpenetrating fluid as a PTM.¹⁹ Although ZIF-8 has been widely studied in the past, most experimental studies upon pressure involve adsorption of guest molecules inside its channels when penetrating PTM are used, making it very challenging to decouple intrinsic pressure-dependent features of the pristine framework from adsorption-induced ones.

In order to elucidate the atomistic origins of these anomalous structural and mechanical features, we performed solid-state quantum-mechanical simulations within the density functional theory (DFT) with the CRYSTAL17 program.³⁴ We first found the optimized lattice parameter of ZIF-8, 17.04 Å, in excellent agreement with the experimental value of 17.0 Å.¹⁹ Additionally, the computed bulk modulus K at zero pressure, 8.9 GPa, is also in excellent agreement with the experimental value of 7.7 GPa, as measured by Brillouin scattering.⁴⁸ We then performed pressure-constrained structural relaxations at 13 pressures in the range 0–0.8 GPa. Figure 1 shows the structure of ZIF-8, with the major structural features involved in the large-amplitude terahertz motions explicitly labeled, as well as the predicted evolution of volume (V) and bulk modulus (K), the latter of which was obtained from the volume–pressure relationship according to $K(P) = -V(P) (\partial P / \partial V)$. As pressure increases, two main structural changes occur. First, a rotation of the imidazolate linking bridges (the “swing-effect” motion), described by the angle φ . Secondly, the ZnN_4 tetrahedra twist, described by the angle θ .

Considering the volume–pressure relationship, Chapman et al. reported the intrinsic structural and mechanical features of pristine ZIF-8 at low pressures using in situ X-ray diffraction and a nonpenetrating fluid as the PTM.¹⁹ The fitting of the experimentally measured data in the 0–0.34 GPa pressure range using a third-order Birch–Murnaghan equation-of-state provided the anomalous negative value for K' of -4.6 . From a theoretical point of view, classical molecular dynamics simulations were unable to confirm this peculiar feature as

they described a bulk modulus almost linearly increasing as a function of pressure in the whole 0–0.4 GPa pressure range and thus a positive value of K' .²⁴ By fitting our simulated volume–pressure data, reported in Figure 1b, in the same pressure range (as experimentally pressures above 0.34 GPa resulted in amorphization, which is not accounted for in our model) and to the same equation-of-state, we get a negative value of $K' = -3.8$, in good agreement with the experimental value. A quantum-mechanical description over a classical one is needed in order to catch such a subtle, and yet fundamental, feature of the mechanical response of ZIF-8, despite such simulations being performed at an effective 0 K temperature.

Let us stress that K' is just an average parameter, which does not reflect the punctual mechanical response of the system at the various pressures. Here, we want to determine the explicit $K(P)$ relation. We perform a more accurate fitting of the pressure–volume data using a higher-than-third-order function (sixth-order polynomial). This fitting allowed us to investigate for the first time the explicit pressure dependence of the bulk modulus of ZIF-8 in that pressure range, which we reported in Figure 1b. Three distinct regions are identified in the volume and bulk modulus: for $P < 0.2$ GPa the $V(P)$ is almost linear, for $P > 0.5$ GPa $V(P)$ is also almost linear, while for pressures $0.2 < P < 0.5$ GPa, the $V(P)$ relation has a sigmoid-shape centered at $P = 0.35$ GPa (i.e., a point where the $K(P)$ relation changes the sign of the slope). Regarding the mechanical properties of ZIF-8, we find that the bulk modulus initially increases up to about 0.1 GPa and then decreases above 0.2 GPa, eventually showing a clear discontinuity at 0.35 GPa. This matches the experimental evidence according to which pressurization beyond 0.34 GPa produces irreversible structural changes leading to the pressure-induced amorphization of the sample possibly due to the disruption of long-range translational symmetry while retaining the short-range order (e.g., local structure and framework connectivity).¹⁹ Again, it is important to make clear that the amorphization observed experimentally is not captured by our model due to the imposition of translational symmetry that prohibits long-range structural disorder; however, the data obtained allow for some insight into the properties of ZIF-8 when amorphization is restricted.

Spectroscopic Fingerprint of Mechanical Softening on Compression. Terahertz spectroscopy has been demonstrated to be an effective technique for probing relevant atomic motions in MOFs.^{8,9,29} However, the assignment of the low-frequency spectrum for the “swing-effect” dynamics in ZIF-8, with peaks at about 1.0 THz (Raman active) and 2.0 THz (infrared active), has been controversial.^{9,29} While a later study has claimed the spectral assignment by Tan et al.²⁹ to be the correct one,³⁰ the results of the present study clearly show that both previously identified peaks indeed correspond to the “swing-effect” motion of the imidazolate linkers (the peak at about 1.0 THz being the symmetric “gate-opening” motion while the peak at about 2.0 THz being the asymmetric “gate-opening” motion). Crucially, this study allows for an explicit correlation of these spectral features with structural and mechanical changes occurring upon external perturbation, in particular upon compression. Note that structural compression in ZIF-8 can be achieved by either increasing the pressure or decreasing the temperature (given that ZIF-8 shows a positive thermal expansion).⁴⁹

We therefore decided to initially investigate the far-IR spectrum of ZIF-8 computationally in the terahertz region at

low pressures, corresponding to the pre-amorphization regime (0.0–0.3 GPa). Figure 2 shows the predicted evolution of the

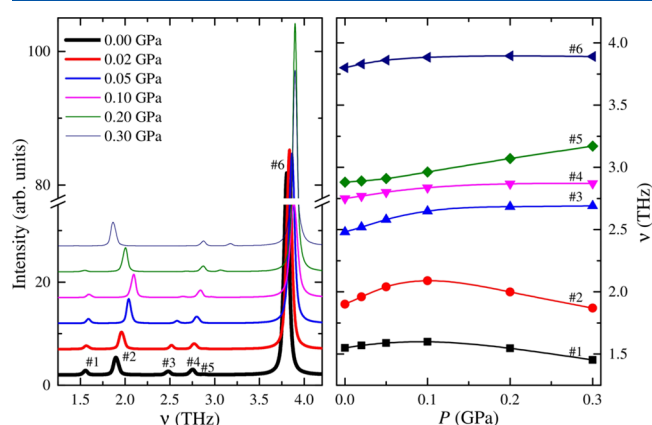


Figure 2. DFT-predicted infrared spectrum of ZIF-8 as a function of pressure (0.0–0.30 GPa) in the terahertz region (left) and the evolution of the IR-active vibrational modes as a function of pressure (right).

infrared spectrum in the terahertz region with increasing pressure. The results highlight that the most peculiar behavior on pressure in this frequency domain is indeed shown by the peak at about 2.0 THz, whose intensity increases and whose position exhibits a remarkable nonlinear shift. This peak is initially blue-shifted with increasing pressure up to about 0.1 GPa and then subsequently red-shifts when pressure is further increased. Thus, this behavior is strictly correlated with the evolution on pressure of the mechanical response of the system discussed above. It also confirms the strong link between the corresponding terahertz lattice dynamics and the structural transformations that ZIF-8 undergoes on pressure. Furthermore, the Raman-active peak at about 1.0 THz also exhibits the same shifting pattern (see Figure S1). This confirms the clear relationship between these spectral features due to symmetric and asymmetric “swing-effect” motions of the imidazolate linkers in the four-membered rings and the mechanochemical properties of ZIF-8. A link to dynamic videos all of the vibrational modes (IR and Raman) of ZIF-8 is provided in the Supporting Information.

We wanted to experimentally confirm the extent to which these spectral features probe the structural changes occurring in ZIF-8 upon perturbation by temperature and pressure. To do this, we have performed a novel pressure- and temperature-dependent THz-TDS experiment, using two different gases as PTM (methane and nitrogen). Figure 3 shows the results for nitrogen; Figure S2 in the Supporting Information shows the results for methane, which are qualitatively similar. First, we observe a significant absorption peak initially near 2.0 THz in the empty ZIF-8, which we refer to as ω^* . This peak is consistent with the previously reported standard THz-TDS result,²⁹ indicating that the sample is crystalline. In that study, this feature was observed to significantly broaden at low temperatures and exhibit an anomalous temperature-induced shifting. In the present study, we clearly observed that as temperature is lowered and structural compression is induced, the frequency of ω^* increased. This was followed by a sudden decrease at about 290 K and 5 bar (Figure 3d), followed by a plateau extending to about 190 K. This feature exhibits the exact same behavior upon compression as predicted by the

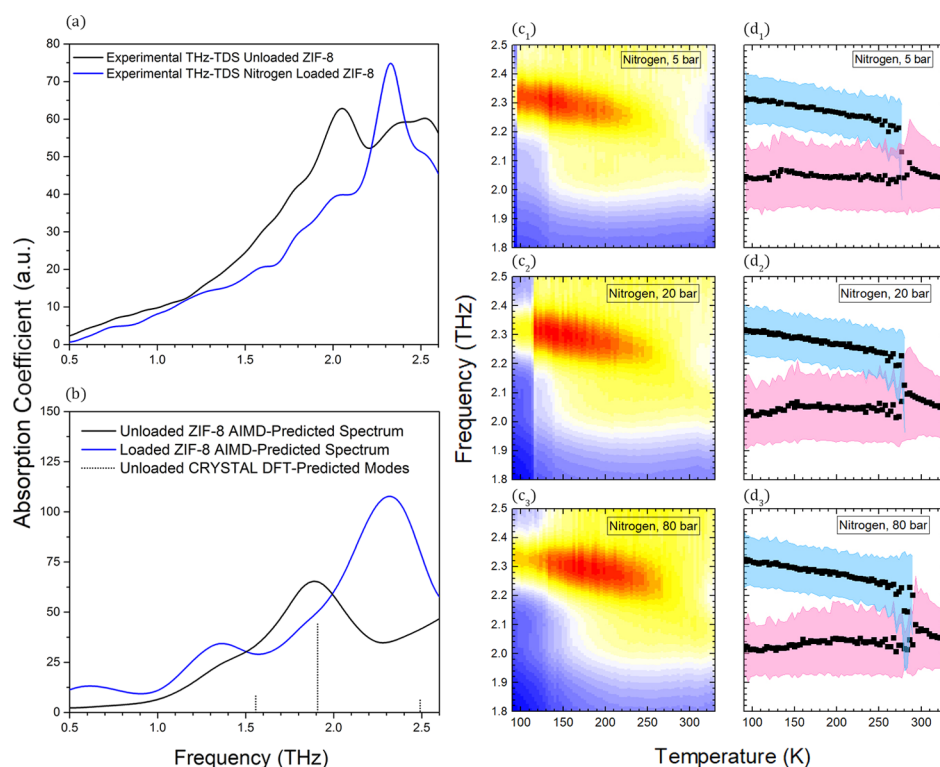


Figure 3. (a) Experimental and (b) AIMD temperature-dependent terahertz absorption spectra at 97 K for ZIF-8 unloaded (black) and loaded with N_2 at 80 bar. The vertical black dotted lines represent the transitions predicted by CRYSTAL17 using static-DFT simulations on a pristine crystal. (c) THz-TDS spectra under varying temperature and pressure, with red and blue colors representing the maximum and minimum of the absorption intensity, respectively; the sharp transitions in (c₁) and (c₂) at 95 and 115 K, respectively, are caused by the change of the refractive index of the sample due to the gas-to-liquid phase transition of nitrogen. (d) Black squares are fitted peak positions while pink and blue shadows are the corresponding line-widths at half-maximum for the peaks at about 2.0 and 2.3 THz, respectively.

quantum-mechanical simulations discussed above (Figure 2); however, it is important to note the range of pressures explored in Figure 2 (0.1 GPa = 1000 bar) and those in Figure 3 (5–80 bar), with the former performed at 0 K and the latter incorporating thermal effects. The discontinuity of ω^* on evolution of temperature, reflected in the change in sign of $\partial\omega^*/\partial T$, shifts to higher temperatures with increasing N_2 pressure, from 288 K at 5 bar to 297 K at 80 bar. Clearly, as the external pressure is increased, a lower degree of thermally induced compression is required to achieve the same overall compression of the structure. These results highlight that the THz-TDS experiments provide a valuable probe of relevant collective structural changes in ZIF-8, in a non-invasive and nondestructive manner.

In addition to the 2.0 THz mode, we further noted that a new spectral peak appears at about 2.3 THz at the exact same temperature at which the structural and mechanical features described above exhibit the discontinuity (Figure 3a,c; Figure 3d) shows this through the blue shaded regions. The origins of this spectral feature are understood in terms of an intrinsic vibrational mode of the framework that is activated by the presence of adsorbed gas molecules in the pores of the solid. Through the use of AIMD simulations, we evaluated the vibrational response of a pristine and loaded (48 nitrogen molecules per cell) ZIF-8 crystal by taking the dipole-moment autocorrelation function of a 30 ps *NVT* trajectory, and the results are shown in Figure 3b. Compared to the pristine (empty) ZIF-8 crystal, an additional feature is clearly predicted in the loaded variant at about 2.3 THz. The “swing-effect” mode at ~ 2 THz is present in both regimes, with the loaded

ZIF-8 presenting a lower intensity for that feature, as observed experimentally (see again Figure 3a). We then deconvolved the spectra into contributions from the host (ZIF-8) and guest (N_2) molecules. We found that the nitrogen molecules did not directly contribute to the low-frequency spectrum of ZIF-8 on their own, but rather dramatically enhance the intensity of an intrinsic spectral feature by breaking a symmetric structural configuration. Indeed, there is a normal mode predicted from the solid-state DFT simulations at about 2.5 THz, which involves a symmetric bending of two imidazolate linkers around a central imidazolate, in a pincer-type motion, which is similar in frequency to both the experimental and AIMD peaks at about 2.3 THz. This mode has a low intensity for the pristine solid because crystallographic symmetry results in the net cancellation of dipole moments for the entire unit cell. However, when the system is loaded, the nitrogen molecules affect this vibration by enabling anisotropic motion through the removal of stringent crystalline symmetry, that is, each imidazolate linker rotates with differing degrees of motion depending on the nitrogen environment, yielding a much larger net change in the dipole moment for the unit cell and thus a greater IR intensity.

Elucidating the Intrinsic-Framework Nature of the High-Pressure Phase Transition with DFT Simulations.

The successful modeling of the structural, dynamical, and mechanical phenomena in the low-pressure regime lends valuable confidence to the theoretical methodology used and enables deeper investigation into the pressure-dependent properties of ZIF-8 to be explored. The observed first-order phase transition at high pressure²⁰ is well-accepted to be

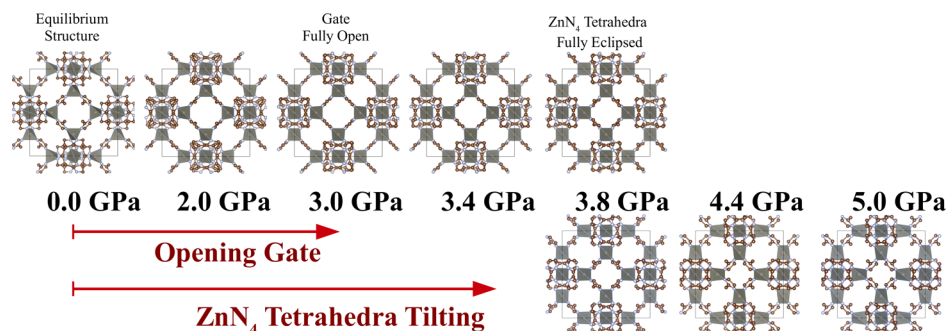


Figure 4. Pressure-induced structural changes through the first-order phase transition and up to 5 GPa in pristine ZIF-8.

assisted by the presence of adsorbed molecules⁵⁰ that are known to play a key role in preventing the amorphization of the framework; however, the role that the ZIF framework alone plays remains unclear. Here, we wanted to understand whether or not the observed phase transition is an intrinsic feature of the pristine ZIF-8 framework or if the transition requires the presence of adsorbed gas molecules, all when amorphization is hindered. Experimentally, amorphization can be hindered at high pressure by the adsorption of guest molecules in the pores; however, performing experiments at high pressure without a PTM is not possible due to the pristine framework undergoing amorphization at pressures above 0.34 GPa,¹⁹ as previously mentioned. Thus, the inherent pressure-dependent properties of the pristine framework at high pressures cannot be captured experimentally. With our theoretical simulations, the crystalline lattice can be preserved also at high pressures by imposing periodic-boundary conditions, which prohibits long-range structural deviations and therefore prohibits amorphization. While this method cannot be confirmed experimentally and without question the results are purely theoretical, understanding how the application of high pressures affects the pristine ZIF-8 framework provides valuable insight into the mechanical response of the solid in the absence of adsorbed gas molecules, an important aspect for understanding MOFs in general. In this sense, the accurate modeling of the low-pressure behavior of ZIF-8 provides some confidence that the forces within the solid are well-reproduced, and thus the data presented here can be considered accurate within the short-range limit.

We therefore wrapped up our study by investigating the pressure-induced structural changes of the pristine ZIF-8 up to 5 GPa using quantum-mechanical simulations with CRYSTAL17. Figure 4 shows the pressure-induced structural changes through the first-order phase transition while the evolution of unit cell volume, φ , and θ as a function of pressure is reported in Figure 5. We first predicted a first-order phase transition (indicated by dashed vertical red lines in Figure 5), which is clearly identified by a sharp discontinuity in all structural features, namely a 1.4% drop in unit cell volume. This is the first evidence of the intrinsic pressure-induced, rather than extrinsic adsorption-induced, nature of the observed first-order phase transition in ZIF-8, although experimentally probing this proves difficult due to the limitation of keeping the solid in its pristine state and avoiding amorphization.

The low-pressure and high-pressure phases of ZIF-8 exhibit the same $I\bar{4}3m$ space group symmetry (i.e., $I\bar{4}3m \rightarrow I\bar{4}3m$), as experimentally reported when using a penetrating PTM. However, the atomistic structural changes characterizing the

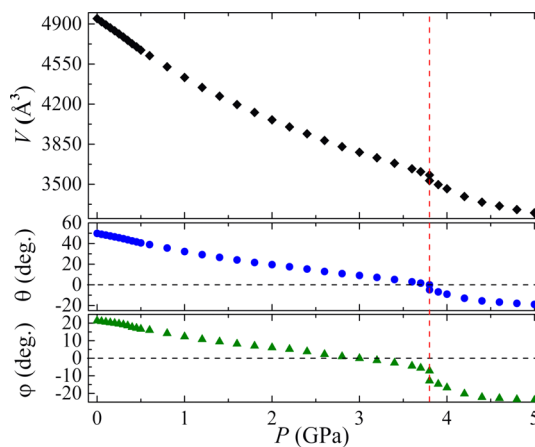


Figure 5. Volume (V), imidazolate linkers “gate-opening” rotation angle (φ), and ZnN_4 tetrahedra tilting angle (θ) as a function of pressure.

phase transition in the pristine ZIF-8 show peculiar features, which differ significantly from those observed experimentally in the loaded system. First, the imidazolate linkers almost linearly rotate as a function of pressure. At zero pressure, they are in a “gate closed” configuration with $\varphi \simeq 20^\circ$, and then, they reach the “gate fully open” configuration with $\varphi = 0^\circ$ at 3.8 GPa, and as pressure further increases, they continue rotating toward another “gate closed” configuration with $\varphi \simeq -20^\circ$. This is quite different with respect to what happens in the relative high-pressure adsorption regime where a high concentration of guest molecules in the pores constrains the linkers to stay “fully open”. Second, in our simulations, the ZnN_4 tetrahedra also tilt almost linearly as a function of pressure, which is not observed experimentally. At zero pressure, $\theta \simeq 50^\circ$, and interestingly in our simulations, the θ angle goes to zero precisely at the predicted transition pressure of 3.8 GPa. The first-order phase transition in pristine ZIF-8 thus occurs when the ZnN_4 tetrahedra are fully eclipsed and the angle θ (rather than the “gate-opening” angle φ) is to be considered the “order parameter” describing the phase transition.

When penetrating PTM are used to convey pressure in the experiments, it is to be expected that the local pressure of the guest molecules acting on the imidazolate linkers would lead to a faster opening of the gate toward a “fully open” configuration, thus allowing more molecules in the pores through the creation of new adsorption sites. In turn, the new adsorption sites help to stabilize the “gate-open” phase. This explains the lower transition pressure observed experimentally for loaded samples with respect to the pristine system. This is further confirmed by the results of the AIMD simulations (vide supra),

which indicate that larger displacements of the linkers occur upon loading.

The results reported in Figure 5 aid in suggesting that the first-order phase transition experimentally observed at 1.47 GPa is due to intrinsic short-ranged structural features of ZIF-8. Because the theoretical application of a hydrostatic pressure alone, with the concomitant imposition of translation symmetry, is able to capture a first order transition that resembles what is observed experimentally, this suggests that long-range effects are not as critical for the phase transition as short-range forces. However, without question the experimentally observed phenomena are different from what is observed here, with the main difference being the adsorbed gas molecules significantly influencing the short-range interactions and thus altering the observed pressure and nature of the phase transition. Regardless, the results presented here, by working within periodic boundary conditions on the pristine system, have demonstrated that the short-range intrinsic structural changes are significant factors in the pressure-induced phase transition in ZIF-8.

CONCLUSIONS

A peculiar nonlinear trend of the mechanochemical response of ZIF-8 as a function of pressure is reported. The bulk modulus of the pristine system increases up to 0.1 GPa of pressure while the system becomes mechanically softer as pressure is further increased up to 0.34 GPa, before undergoing amorphization. The combination of experimental pressure- and temperature-dependent THz TDS and quantum mechanical simulations allows for an atomistic characterization of the static structural changes and dynamic collective lattice vibrations responsible for this behavior. The explicit connection between symmetric and asymmetric “gate-opening” motions of the imidazolate linkers in the four-membered rings of the ZIF-8 framework and its mechanical response is reported. These low-frequency collective vibrations are probed experimentally with THz-TDS as a function of structural compression, and a clear correlation is reported with the corresponding mechanical response on pressure. The methodology presented here can be applied to any supramolecular material. The short-ranged intrinsic nature of the high-pressure first-order phase transition of ZIF-8 is unveiled.

ASSOCIATED CONTENT

Supporting Information

The Supporting Information is available free of charge on the ACS Publications website at DOI: 10.1021/acs.jpcc.8b08334.

INPUT files for crystal (PDF)

Pressure-dependent structural change in ZIF-8 (MOV)

Pressure dependence of IR- and Raman-active “swing-effect” mode, pressure-dependent experimental THz-TDS data using methane as the PTM, and the vibrational modes of ZIF-8 can be visualized on the following webpage http://www.crystal.unito.it/vibs/ZIF-8_under_pressure/index.html?name=zif8_m062x_0.0gpa_freq.xyz (PDF)

AUTHOR INFORMATION

Corresponding Authors

*E-mail: alessandro.erba@unito.it (A.E.).

*E-mail: michael.ruggiero@uvm.edu. Phone: +1 (802) 656-0276 (M.T.R.).

ORCID

Jefferson Maul: 0000-0002-4920-1001

David Fairen-Jimenez: 0000-0002-5013-1194

Daniel M. Mittleman: 0000-0003-4277-7419

J. Axel Zeitler: 0000-0002-4958-0582

Alessandro Erba: 0000-0002-2986-4254

Michael T. Ruggiero: 0000-0003-1848-2565

Author Contributions

[#]W.Z. and J.M. contributed equally.

Notes

The authors declare no competing financial interest.

ACKNOWLEDGMENTS

M.T.R. thanks the University of Vermont for support. M.T.R. and J.A.Z. thank the UK Engineering and Physical Sciences Research Council for funding (EP/N022769/1), and via our membership of the UK's HEC Materials Chemistry Consortium, which is funded by EPSRC (EP/L000202), this work used the ARCHER UK National Supercomputing Service (<http://www.archer.ac.uk>). W.Z. and D.M.M. thank the R. A. Welch Foundation for funding. A.E. and J.M. thank the University of Torino and the Compagnia di San Paolo for funding (CSTO169372). This project has received funding from the European Research Council (ERC) under the European Union's Horizon 2020 research and innovation programme (NanoMOFdeli), ERC-2016-COG 726380. D.F.J. thanks the Royal Society for funding through a University Research Fellowship.

REFERENCES

- (1) Goodwin, A. L.; Kepert, C. J. Negative Thermal Expansion And Low-Frequency Modes in Cyanide-Bridged Framework Materials. *Phys. Rev. B: Condens. Matter Mater. Phys.* **2005**, *71*, 140301.
- (2) Zhou, W.; Wu, H.; Yildirim, T.; Simpson, J. R.; Walker, A. R. H. Origin of the Exceptional Negative Thermal Expansion in Metal-Organic Framework-5 $Zn_4O(1,4\text{-benzenedicarboxylate})_3$. *Phys. Rev. B: Condens. Matter Mater. Phys.* **2008**, *78*, 054114.
- (3) Brozek, C. K.; Michaelis, V. K.; Ong, T.-C.; Bellarosa, L.; López, N.; Griffin, R. G.; Dinçã, M. Dynamic DMF Binding in MOF-5 Enables the Formation of Metastable Cobalt-Substituted MOF-5 Analogues. *ACS Cent. Sci.* **2015**, *1*, 252–260.
- (4) Van Yperen-De Deyne, A.; Hendrickx, K.; Vanduyfhuys, L.; Sastre, G.; Van Der Voort, P.; Van Speybroeck, V.; Hemelsoet, K. Vibrational Fingerprint of the Absorption Properties of UiO-Type MOF Materials. *Theor. Chem. Acc.* **2016**, *135*, 102.
- (5) Turton, D. A.; Senn, H. M.; Harwood, T.; Laphorn, A. J.; Ellis, E. M.; Wynne, K. Terahertz Underdamped Vibrational Motion Governs Protein-Ligand Binding in Solution. *Nat. Commun.* **2014**, *5*, 3999.
- (6) Gerstman, B.; Roberson, M.; Austin, R. Enhancement of Ligand Binding to Myoglobin By Far-Infrared Excitation From a Free-Electron Laser. *J. Opt. Soc. Am. B* **1989**, *6*, 1050–1057.
- (7) Ruggiero, M. T.; Krynski, M.; Kissi, E. O.; Sibik, J.; Markl, D.; Tan, N. Y.; Arslanov, D.; van der Zande, W.; Redlich, B.; Korter, T. M.; et al. The Significance of the Amorphous Potential Energy Landscape For Dictating Glassy Dynamics and Driving Solid-State Crystallisation. *Phys. Chem. Chem. Phys.* **2017**, *19*, 30039–30047.
- (8) Ryder, M. R.; Civalleri, B.; Cinque, G.; Tan, J.-C. Discovering Connections between Terahertz Vibrations and Elasticity Under-Pinning the Collective Dynamics of the HKUST-1 Metal-Organic Framework. *CrystEngComm* **2016**, *18*, 4303–4312.
- (9) Ryder, M. R.; Civalleri, B.; Bennett, T. D.; Henke, S.; Rudić, S.; Cinque, G.; Fernandez-Alonso, F.; Tan, J.-C. Identifying the Role of Terahertz Vibrations in Metal-Organic Frameworks: From Gate-

Opening Phenomenon to Shear-Driven Structural Destabilization. *Phys. Rev. Lett.* **2014**, *113*, 215502.

(10) Mason, J. A.; Oktawiec, J.; Taylor, M. K.; Hudson, M. R.; Rodriguez, J.; Bachman, J. E.; Gonzalez, M. I.; Cervellino, A.; Guagliardi, A.; Brown, C. M.; et al. Methane Storage in Flexible Metal-Organic Frameworks with Intrinsic Thermal Management. *Nat. Commun.* **2015**, *5*, 27, 357–361.

(11) Zhuang, J.; Kuo, C.-H.; Chou, L.-Y.; Liu, D.-Y.; Weerapana, E.; Tsung, C.-K. Optimized Metal-Organic-Framework Nanospheres For Drug Delivery: Evaluation of Small-Molecule Encapsulation. *ACS Nano* **2014**, *8*, 2812–2819.

(12) Rogge, S. M. J.; Bavykina, A.; Hajek, J.; Garcia, H.; Olivos-Suarez, A. I.; Sepúlveda-Escribano, A.; Vimont, A.; Clet, G.; Bazin, P.; Kapteijn, F.; et al. Metal-Organic And Covalent Organic Frameworks As Single-Site Catalysts. *Chem. Soc. Rev.* **2017**, *46*, 3134–3184.

(13) Miralda, C. M.; Macias, E. E.; Zhu, M.; Ratnasamy, P.; Carreon, M. A. Zeolitic Imidazole Framework-8 Catalysts in the Conversion of CO₂ to Chloropropene Carbonate. *ACS Catal.* **2012**, *2*, 180–183.

(14) Koyuturk, B.; Altintas, C.; Kinik, F. P.; Keskin, S.; Uzun, A. Improving Gas Separation Performance of ZIF-8 by [BMIM][BF₄] Incorporation: Interactions and Their Consequences on Performance. *J. Phys. Chem. C* **2017**, *121*, 10370–10381.

(15) Furukawa, H.; Cordova, K. E.; O’Keeffe, M.; Yaghi, O. M. The Chemistry And Applications of Metal-Organic Frameworks. *Science* **2013**, *341*, 1230444.

(16) Moghadam, P. Z.; Li, A.; Wiggin, S. B.; Tao, A.; Maloney, A. G. P.; Wood, P. A.; Ward, S. C.; Fairen-Jimenez, D. Development of a Cambridge Structural Database Subset: A Collection of Metal-Organic Frameworks for Past, Present, and Future. *Chem. Mater.* **2017**, *29*, 2618–2625.

(17) Wilmer, C. E.; Leaf, M.; Lee, C. Y.; Farha, O. K.; Hauser, B. G.; Hupp, J. T.; Snurr, R. Q. Large-Scale Screening of Hypothetical Metal-Organic Frameworks. *Nat. Chem.* **2012**, *4*, 83–89.

(18) Bux, H.; Liang, F.; Li, Y.; Cravillon, J.; Wiebcke, M.; Caro, J. Zeolitic Imidazolate Framework Membrane with Molecular Sieving Properties By Microwave-Assisted Solvothermal Synthesis. *J. Am. Chem. Soc.* **2009**, *131*, 16000–16001.

(19) Chapman, K. W.; Halder, G. J.; Chupas, P. J. Pressure-Induced Amorphization and Porosity Modification in a Metal–Organic Framework. *J. Am. Chem. Soc.* **2009**, *131*, 17546–17547.

(20) Moggach, S. A.; Bennett, T. D.; Cheetham, A. K. The Effect of Pressure on ZIF-8: Increasing Pore Size with Pressure and the Formation of a High-Pressure Phase at 1.47 GPa. *Angew. Chem., Int. Ed.* **2009**, *48*, 7087–7089.

(21) Fairen-Jimenez, D.; Moggach, S. A.; Wharmby, M. T.; Wright, P. A.; Parsons, S.; Düren, T. Opening the Gate: Framework Flexibility in ZIF-8 Explored by Experiments and Simulations. *J. Am. Chem. Soc.* **2011**, *133*, 8900–8902.

(22) Zhang, L.; Hu, Z.; Jiang, J. Sorption-Induced Structural Transition of Zeolitic Imidazolate Framework-8: A Hybrid Molecular Simulation Study. *J. Am. Chem. Soc.* **2013**, *135*, 3722–3728.

(23) Im, J.; Yim, N.; Kim, J.; Vogt, T.; Lee, Y. High-pressure Chemistry of a Zeolitic Imidazolate Framework Compound in the Presence of Different Fluids. *J. Am. Chem. Soc.* **2016**, *138*, 11477–11480.

(24) Ortiz, A. U.; Boutin, A.; Fuchs, A. H.; Coudert, F.-X. Investigating the Pressure-Induced Amorphization of Zeolitic Imidazolate Framework ZIF-8: Mechanical Instability Due to Shear Mode Softening. *J. Phys. Chem. Lett.* **2013**, *4*, 1861–1865.

(25) Hobday, C. L.; Woodall, C. H.; Lennox, M. J.; Frost, M.; Kamenev, K.; Düren, T.; Morrison, C. A.; Moggach, S. A. Understanding the Adsorption Process in ZIF-8 Using High Pressure Crystallography And Computational Modelling. *Nat. Commun.* **2018**, *9*, 1429.

(26) Casco, M. E.; Cheng, Y. Q.; Daemen, L. L.; Fairen-Jimenez, D.; Ramos-Fernández, E. V.; Ramirez-Cuesta, A. J.; Silvestre-Albergo, J. Gate-opening Effect in ZIF-8: The First Experimental Proof Using Inelastic Neutron Scattering. *Chem. Commun.* **2016**, *52*, 3639–3642.

(27) Coudert, F.-X. Molecular Mechanism of Swing Effect in Zeolitic Imidazolate Framework ZIF-8: Continuous Deformation upon Adsorption. *ChemPhysChem* **2017**, *18*, 2732–2738.

(28) Ruggiero, M. T.; Bardon, T.; Strlič, M.; Taday, P. F.; Korter, T. M. The Role of Terahertz Polariton Absorption in the Characterization of Crystalline Iron Sulfate Hydrates. *Phys. Chem. Chem. Phys.* **2015**, *17*, 9326–9334.

(29) Tan, N. Y.; Ruggiero, M. T.; Orellana-Tavra, C.; Tian, T.; Bond, A. D.; Korter, T. M.; Fairen-Jimenez, D.; Zeitler, J. A. Investigation of the Terahertz Vibrational Modes of ZIF-8 and ZIF-90 with Terahertz Time-Domain Spectroscopy. *Chem. Commun.* **2015**, *51*, 16037–16040.

(30) Tanno, T.; Watanabe, Y.; Umeno, K.; Matsuoka, A.; Matsumura, H.; Odaka, M.; Ogawa, N. In Situ Observation of Gas Adsorption onto ZIF-8 Using Terahertz Waves. *J. Phys. Chem. C* **2017**, *121*, 17921–17924.

(31) Parrott, E. P. J.; Zeitler, J. A. Terahertz Time-Domain And Low-Frequency Raman Spectroscopy of Organic Materials. *Appl. Spectrosc.* **2015**, *69*, 1–25.

(32) Elcombe, M. M.; Pryor, A. W. The Lattice Dynamics of Calcium Fluoride. *J. Phys. C: Solid State Phys.* **1970**, *3*, 492–499.

(33) Freire, J. D.; Katiyar, R. S. Lattice Dynamics of Crystals with Tetragonal BaTiO₃ Structure. *Phys. Rev. B: Condens. Matter Mater. Phys.* **1988**, *37*, 2074–2085.

(34) Dovesi, R.; Erba, A.; Orlando, R.; Zicovich-Wilson, C. M.; Civalleri, B.; Maschio, L.; Rérat, M.; Casassa, S.; Baima, J.; Salustro, S.; et al. Quantum-Mechanical Condensed Matter Simulations with Crystal. *Wiley Interdiscip. Rev.: Comput. Mol. Sci.* **2018**, *8*, No. e1360.

(35) Zhao, Y.; Truhlar, D. G. The M06 Suite of Density Functionals for Main Group Thermochemistry, Thermochemical Kinetics, Noncovalent Interactions, Excited States, and Transition Elements: Two New Functionals and Systematic Testing of Four M06-Class Functionals and 12 Other Functionals. *Theor. Chem. Acc.* **2007**, *120*, 215–241.

(36) Zhu, A.-X.; Lin, R.-B.; Qi, X.-L.; Liu, Y.; Lin, Y.-Y.; Zhang, J.-P.; Chen, X.-M. Zeolitic Metal Azolate Frameworks (MAFs) from ZnO/Zn(OH)₂ and Monoalkyl-Substituted Imidazoles and 1,2,4-Triazoles: Efficient Syntheses and Properties. *Microporous Mesoporous Mater.* **2012**, *157*, 42–49.

(37) Erba, A.; Mahmoud, A.; Belmonte, D.; Dovesi, R. High Pressure Elastic Properties of Minerals From Ab Initio Simulations: The Case of Pyrope, Grossular And Andradite Silicate Garnets. *J. Chem. Phys.* **2014**, *140*, 124703.

(38) Zicovich-Wilson, C. M.; Pascale, F.; Roetti, C.; Saunders, V. R.; Orlando, R.; Dovesi, R. Calculation of the Vibration Frequencies of α -Quartz: The Effect of Hamiltonian and Basis Set. *J. Comput. Chem.* **2004**, *25*, 1873–1881.

(39) Hutter, J.; Iannuzzi, M.; Schiffrmann, F.; VandeVondele, J. cp2k: Atomistic Simulations of Condensed Matter Systems. *Wiley Interdiscip. Rev.: Comput. Mol. Sci.* **2013**, *4*, 15–25.

(40) Nosé, S. A Unified Formulation of the Constant Temperature Molecular Dynamics Methods. *J. Chem. Phys.* **1998**, *81*, 511–519.

(41) Perdew, J. P.; Burke, K.; Ernzerhof, M. Generalized Gradient Approximation Made Simple. *Phys. Rev. Lett.* **1996**, *77*, 3865–3868.

(42) VandeVondele, J.; Hutter, J. Gaussian Basis Sets For Accurate Calculations On Molecular Systems in Gas And Condensed Phases. *J. Chem. Phys.* **2007**, *127*, 114105.

(43) Goedecker, S.; Teter, M.; Hutter, J. Separable Dual-space Gaussian Pseudopotentials. *Phys. Rev. B: Condens. Matter Mater. Phys.* **1996**, *54*, 1703–1710.

(44) Grimme, S.; Antony, J.; Ehrlich, S.; Krieg, H. A Consistent and Accurate Ab Initio Parametrization of Density Functional Dispersion Correction (DFT-D) for the 94 Elements H-Pu. *J. Chem. Phys.* **2010**, *132*, 154104.

(45) Brehm, M.; Kirchner, B. Travis—a Free Analyzer and Visualizer for Monte Carlo and Molecular Dynamics Trajectories. *J. Chem. Inf. Model.* **2011**, *51*, 2007–2023.

(46) Ruggiero, M. T.; Zeitler, J. A. Resolving the Origins of Crystalline Anharmonicity Using Terahertz Time-domain Spectros-

copy and ab initio Simulations. *J. Phys. Chem. B* **2016**, *120*, 11733–11739.

(47) Zhang, W.; Nickel, D.; Mittleman, D. High-Pressure Cell For Terahertz Time-Domain Spectroscopy. *Opt. Express* **2017**, *25*, 2983–2993.

(48) Tan, J.-C.; Civalleri, B.; Lin, C.-C.; Valenzano, L.; Galvelis, R.; Chen, P.-F.; Bennett, T. D.; Mellot-Draznieks, C.; Zicovich-Wilson, C. M.; Cheetham, A. K. Exceptionally Low Shear Modulus in a Prototypical Imidazole-Based Metal-Organic Framework. *Phys. Rev. Lett.* **2012**, *108*, 095502.

(49) du Bourg, L. B.; Ortiz, A. U.; Boutin, A.; Coudert, F.-X. Thermal And Mechanical Stability of Zeolitic Imidazolate Frameworks Polymorphs. *APL Mater.* **2014**, *2*, 124110.

(50) Fairen-Jimenez, D.; Galvelis, R.; Torrisi, A.; Gellan, A. D.; Wharmby, M. T.; Wright, P. A.; Mellot-Draznieks, C.; Düren, T. Flexibility and Swing Effect on the Adsorption of Energy-Related Gases on ZIF-8: Combined Experimental and Simulation Study. *Dalton Trans.* **2012**, *41*, 10752–10762.